Accepted Manuscript

Calorimetric study and microstructure analysis of the order-disorder phase transformation in silicon steel built by SLM

J.N. Lemke, M. Simonelli, M. Garibaldi, I. Ashcroft, R. Hague, M. Vedani, R. Wildman, C. Tuck

PII: S0925-8388(17)32073-X

DOI: 10.1016/j.jallcom.2017.06.085

Reference: JALCOM 42154

To appear in: *Journal of Alloys and Compounds*

Received Date: 21 April 2017

Accepted Date: 7 June 2017

Please cite this article as: J.N. Lemke, M. Simonelli, M. Garibaldi, I. Ashcroft, R. Hague, M. Vedani, R. Wildman, C. Tuck, Calorimetric study and microstructure analysis of the order-disorder phase transformation in silicon steel built by SLM, *Journal of Alloys and Compounds* (2017), doi: 10.1016/j.jallcom.2017.06.085.

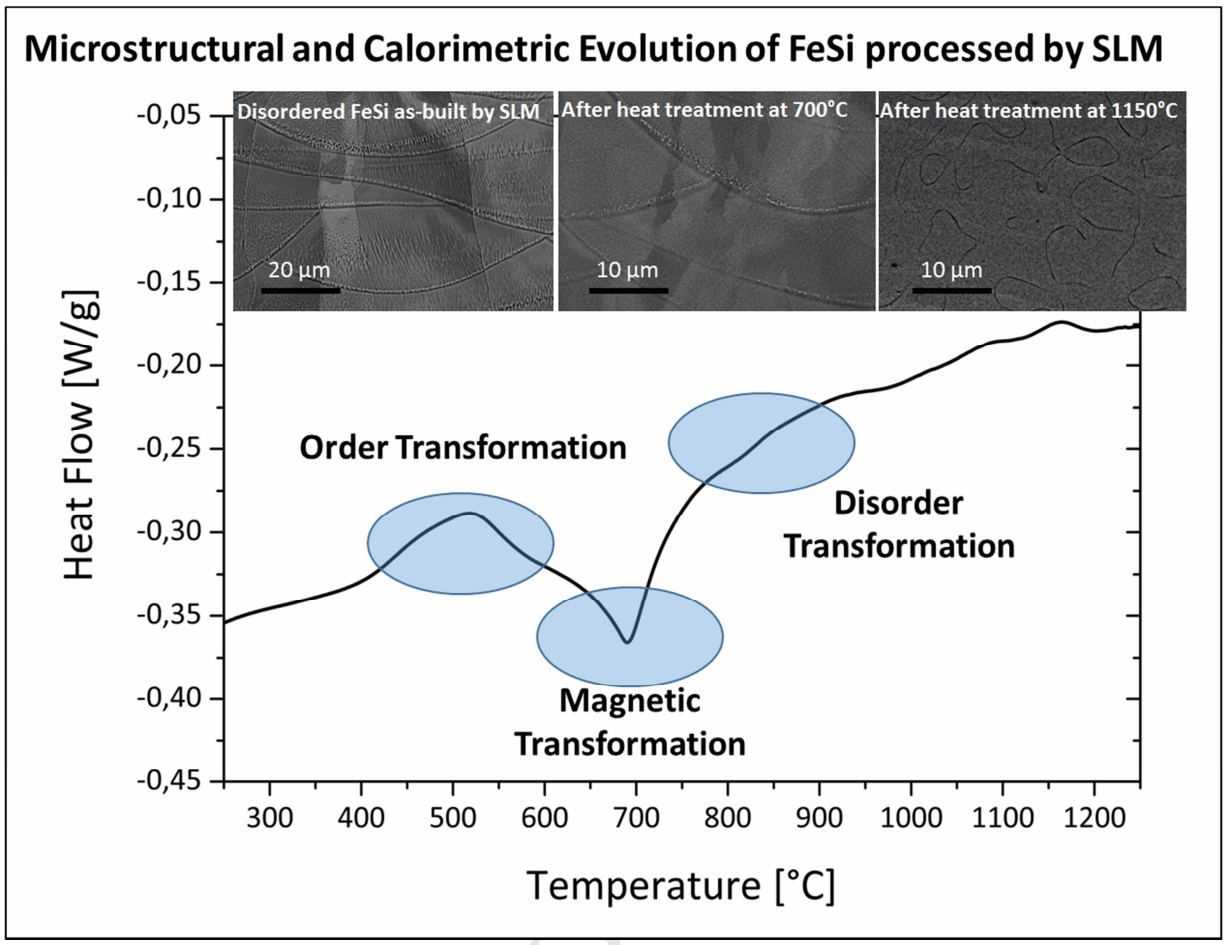
Microstructural and Calorimetric Evolution of FeSi processed by SLM
Disordered FeSi as-built by SLM
After heat treatment at 700°C
After heat treatment at 1150°C
20 µm
10 µm
10 µm
Heat Flow [W/g]
-0,05
-0,10
-0,15
-0,20
-0,25
-0,30
-0,35
-0,40
-0,45
Order Transformation
Disorder Transformation
Magnetic Transformation
300
400
500
600
700
800
900
1000
1100
1200
Temperature [°C]

Calorimetric study and microstructure analysis of the order-disorder phase transformation in silicon steel built by SLM

J. N. Lemke[a], M. Simonelli[b], M. Garibaldi[b], I. Ashcroft[b], R. Hague[b], M. Vedani[a], R. Wildman[b], C.Tuck[b]

[a]Department of Mechanical Engineering, Politecnico di Milano, Via La Masa 1, 20156 Milan, Italy.
[b]Additive Manufacturing and 3D Printing Research Group, Faculty of Engineering, The University of Nottingham, Nottingham NG7 2RD, United Kingdom.

Abstract

Innovative Additive Manufacturing (AM) technologies like Selective Laser Melting (SLM) could prove to be efficient for the processing of brittle silicon steel (Fe-Si) with high silicon content. This research elucidates the effects of heat-treatment on the microstructure of SLM-built high silicon steel, with particular emphasis on the formation of ordered phases, which are known to cause undesired material embrittlement.
Silicon steel with 6.9 wt. % Si is produced by SLM and investigated performing Differential Scanning Calorimetry (DSC), microstructure analysis and hardness measurements. As-built Fe-Si parts are found to consist primarily of disordered A2 phase as the high cooling rates typical of SLM suppress the ordering phase transformations. It is shown how heat treatments can be applied to modify the state of ordering and morphology of the rapidly solidified microstructure. By shedding light on the phase-ordering mechanisms and the effect of heat treatments on microstructure of high-Si steel built by SLM, the present study paves the way towards the optimisation of the mechanical and magnetic properties of this alloy.

Keywords: Selective Laser Melting (SLM), Differential Scanning Calorimetry (DSC), microstructure, silicon steel, heat-treatment, ordering phase transformations

Introduction

Silicon steels are one of the most important classes of materials for magnetic applications as they are widely used in transformer cores, electric motors and generators. Fe-Si alloys, based on no other alloying element than Si, are not easy to process: they exhibit a low workability and they become increasingly brittle as Si is progressively added [1]. On the other hand, a high amount of Si is favourable for soft magnetic applications as this guarantees low magnetostriction, suppresses magnetocrystalline anisotropy and increases the electrical resistivity of the alloy [2]. Because of its limited workability, commercial Fe-Si for industrial applications is commonly fabricated at Si contents not exceeding 3 wt. %, although it has been proposed that the best composition for

magnetic properties lies around 6.5 wt. % [2, 3]. Producing silicon steel at such elevated Si content has been reported using rapid quenching for the production of thin ribbons [4], chemical vapour deposition [5] and spray forming [6].

High silicon Fe-Si is bcc-structured over the whole solid temperature range. The structure of fully annealed specimens is indicated in the Fe-Si binary phase diagram shown in Figure 1 [7].

Figure 1 Region of interest of the Fe-Si phase diagram (as designed by Swann et al.) and atomic structures of the ordered phases B2 and $D0_3$ [7]

Cooling from the melt, the material undergoes two ordering phase transitions, i.e. transformations that involve the re-arrangement of Si in the Fe lattice. The first disorder-order transformation is located at around 820°C. Disordered ferritic solid solution, commonly referred to as A2, transforms into a short range ordered B2 phase, with the previously randomly distributed Si atoms now occupying the centre position of the bcc cells, with Fe atoms located at the cell corners [8]. The B2 phase has a stoichiometry of 1:1 Fe to Si atoms, consequentially Fe-Si at 6.9 wt. % Si can only be partially B2 ordered. Cooling further, the material exhibits a magnetic transition around 680°C. At this temperature the randomized magnetic spins align spontaneously and the material becomes ferromagnetic [9]. A further ordering transformation takes place at a temperature below 650°C. The B2 phase and some of the residual A2 transform into B2+$D0_3$. The stoichiometry of $D0_3$ is 1:2, with the centre position of every second bcc cell occupied by a Si atom. This ordering can attain much further extension in this phase region in comparison to the B2 [8]. The ordering arrangement of the solute affects several physical properties of the high silicon steels and has negative implications. While it is not established how the ordered domains affect the electrical/magnetic properties of the alloy, it is well known that ordering increases the hardness and hence the brittleness of the material, reducing drastically its workability [10, 11].

As recently demonstrated, Selective Laser Melting (SLM) is a promising additive manufacturing technique that may extend the manufacturing envelope of high silicon steels with arbitrary shapes, high integrity and controllable grain orientation [12]. In addition, it has been shown through preliminary XRD studies that the high cooling rates involved in the scan process could hinder the described ordering transformations and thus, in principle, improve the mechanical properties. Building on the findings in [12], the aim of the present contribution is to shed light on the effects of heat-treatment on the microstructures of SLM-built Fe-Si, with particular regards to the state of ordering. Differential Scanning Calorimetry (DSC) combined with SEM and Vickers

hardness is used to gain insights into the phase transformations in this material. Although ordering has been investigated in the literature by TEM [13, 14], XRD [6, 13], Mössbauer spectroscopy [15] and neutron diffraction [16], characterizing ordering transitions remains challenging as these techniques require high expertise and give only partial insight about ordering state and quantity of ordered phases in the material. The accessibility and the abundance of information extractable from DSC measurements could make this method a powerful complementary tool for the characterisation of the structure of materials undergoing ordering transformations [9, 17].

Methods and material

Gas atomized, pre-alloyed Fe-Si powders with a neat size distribution within 10 and 60 µm were supplied by LPW Technology Ltd. The silicon steel contains 6.9 wt. % Si with a few traces of C, Mn, P and O which were limited during production to an amount that is not considered to affect the mechanical and magnetic properties of final parts. The chemical composition is presented in Table 1.

Table 1 Composition of Fe-Si powders

A Realizer SLM-50 system operating with a protective Ar atmosphere and an oxygen level below 0.4% and equipped with a 100 W yttrium fibre laser which scans continuous tracks was used to produce Fe-Si cubes of 5 × 5 × 5 mm dimension. The build platform was preheated to 200°C to reduce thermal gradients during processing. A bidirectional scanning strategy whereby the scan direction was rotated by 90° on each layer was used to perform three builds of nine cubes, each supported by 3 mm secondary support structures that could be easily removed at the end of the process. Parameters were selected based on a preliminary optimisation to minimise cracking and porosity. The relative density of cubes was measured to be above 98% [12]. Table 2 reports the applied laser parameters.

Table 2 Selected build parameters for processing of Fe-Si cubic specimens

The calorimetric study was carried out on the feedstock powders, as-built specimens and specimens exposed to various heat treatments in order to modify microstructure according to the Fe-Si phase diagram shown in Figure 1. Heat treatments were chosen in regions of the phase diagram that are of interest for analytical purposes, i.e. for microstructure, stress relief and grain growth analysis. A heat treatment at 400°C was selected with two different dwell

times to investigate the ordering behaviour at low temperatures where diffusion is low and the ordering reaction may proceed slowly. Heat treatments at 620°C, 700°C and 900°C were performed to induce B2+$D0_3$, B2 and A2 phase transitions, respectively. The first treatment was also performed with 5 hours dwell time in order to validate whether after one hour the maximum amount of ordering is induced, the latter two treatments with subsequent water quenching were in order to prevent further microstructural transformations upon cooling. A high temperature treatment at 1150° was selected to normalize the microstructure and investigate the effect of grain growth [17, 18]. The investigated heat treatments are reported in Table 3, together with the predicted phase regions.

Table 3 Overview of the investigated Fe-Si samples. The cooling method, annealing temperature, dwell time and the region of the phase diagram covered by the heat treatment are presented in the Table.

To simplify the discussion, the following nomenclature will be used. As-received gas atomized Fe-Si powders are indicated as sample 'P'. The parts printed by SLM in the as-built condition are referred to as 'AsB'. The printed samples that were annealed at different temperatures but fixed dwell time of 1 h followed by furnace cooling are denoted by 'A' and a number representing the annealing temperature. Samples which deviate from these heat cycles, either because they underwent extended annealing times or quenching are denoted with 'Ex' and 'Q', respectively.

A precision cutting tool "Brilliant 220" by ATM was used to cut samples. Cubes were sectioned along the centre x-y and x-z planes to produce four samples of equal size which were then heat treated. The as-built and heat treated samples for microstructural analysis were subsequently prepared using standard metallurgical methods. Mechanical grinding and polishing were performed using abrasive paper and diamond paste down to 1 µm. The samples were then polished for a further 20 minutes with colloidal Silica and etched with Nital 2% to reveal the ferritic grain structure and the SLM scan track features. The x-y plane was selected for the microstructure investigations as the Fe-Si samples showed a significant anisotropy in the build direction, with a strong dependence on the laser parameters [12]. Microstructural images were taken with a LV100ND optical microscope and a TM3030 SEM operating in back-scatter mode. Microstructural planes are referred to according to the conventions in ISO ASTM 52 921: 2013 [19], where x-y is the transversal plane (plane scanned by the laser) and x-z/y-z are the lateral planes of the built Fe-Si cubes (z-direction is parallel to the build direction). Grain size was measured using the linear intercept method along at least three arbitrary straight lines for each condition.

Alumina pans were used as sample holders and as a reference crucible to record DSC heating curves using samples with weights in the range of 50 and 150 mg on a SDT Q600 DSC device by TA instruments, working in an Ar atmosphere. Sample pans were cleaned in an ultra-sonic bath for 3 min before calorimetric measurements. The heating and cooling rate was set to 30°C/min. DSC curves were plotted subtracting the recorded baselines. In order to guarantee reproducibility, DSC heating curves were recorded for four samples in the AsB condition. A Buehler Micro Vickers indenter was used to measure hardness, recording 5 values each on the x-z and x-y planes in the centre of the cut sample cubes.

Results and discussion

Microstructural features in the as-built specimens

The microstructure of Si-Fe as-built by SLM is shown in Figure 2.

Figure 2 Representative SEM micrographs of Fe-Si as-built by SLM: a) x-y plane, low magnification, b) x-y plane, high magnification, c) x-z plane, low magnification, d) x-z plane and high magnification. In low magnification images red arrows mark the scanning direction. The scanning direction parallel to the y-axis is indicated by red crosses.

Ferritic grains can be identified by regions of equal brightness in the SEM images as the grain – electron beam relative orientation affects the apparent density and causes different contrast. The microstructure is characterised by continuous melt pools which span a width of approximately 90 - 100 µm and superpose the ferritic grains. It is possible to observe the effect of the bidirectional scanning strategy especially in the low magnification images, where scan tracks of every second layer run parallel (red markings on the SEM micrographs of Figure 2a and c). Higher magnification images (Figure 2b and 2d) reveal the cellular structure which appears larger close to the melt pool boundaries. Micrographs are presented here to facilitate the following discussion, a detailed research work on the microstructure of SLM high silicon Fe-Si has been recently published in a related work [12].

Microstructural evolution during heat treatments at increasing temperatures

Samples were studied by optical microscopy before etching in order to evaluate the grain size without the superposition by the SLM melt-pool features on the ferrite grain structure. The evolution of grain size following the various heat treatments is illustrated in Figure 3.

Figure 3 Optical micrographs of selected unetched heat treated samples: a) AsB, b) A700, c) A900, and d) A1150. Some of the defects are marked by red arrows

Some pores were observed in the micrographs, principally caused by insufficient melting. The variation in number of defects shown in the micrographs of Figure 3 are not expected to be representative for the total amount of defects as samples density produced with selected parameters did not differ significantly [12]. The average grain size of the as-built samples, AsB, (Figure 3a) was below 100 µm. No grain growth occurred up to heat treatments in the B2 region of the phase diagram as observed by the comparison of the as-built samples and those annealed for 1 h at 700°C, Figure 3b. Neither did the grains show any significant growth during the annealing at 900°C (Figure 3c) for 1 h. Similar research conducted on microcrystalline Fe-Si ribbons reported a low amount of grain growth at 900°C, however this reference data was reported for heat treatments lasting 24 h [18]. Annealing conducted at 1150°C for 1 h, caused instead a marked grain growth, with grains increasing by up to around 100 µm in dimension as shown in Figure 3d. The evolution of the microstructure following heat treatments in the B2+$D0_3$, B2 and A2 regions is shown in Figure 4.

Figure 4 SEM micrographs representing microstructural evolution of samples after annealing for 1 h at: a) 620°C, b) 700°C, c) 900°C, d) 900°C with subsequent quenching. The 400°C annealed condition is not presented here as by SEM analysis the microstructure seemed identical to as-built

No distinct microstructural differences are noted after annealing in the B2+$D0_3$ region (treatment A400 and A620). Considering the phase diagram, A620 should lead to the formation of a significant amount of ordering compared to the predominately disordered as-built specimens, but the microstructure at the microscale seems unaltered (Figure 4a). Figure 4b presents the microstructure after an annealing in the B2 region at 700°C for 1 h. The typical microstructural features induced by SLM, such as melt pool boundaries and cells, are partly dissolved and appear discontinuous. It is believed, that at this temperature the diffusion rate is just sufficient to bring Si segregations into solid solution. After heat treating the samples in the A2 region at 900°C for 1 h, the SLM induced structure dissolved completely, i.e. the cells and melt pool segregations entered into solid solution. Upon slow furnace cooling, the silicon segregated again, resulting in a fine structure overlaying the ferritic grains (Figure 4c). This is confirmed by the microstructure of Q900 (Figure 4d), as quenching after heat treating at 900°C, allows Si to be kept in solid solution and the resulting microstructure is homogenous. Annealing at elevated temperatures in the A2 region, followed by furnace cooling, led to a complete dissolution of segregations and homogenisation of microstructure, as shown in Figure 5.

Figure 5 Representative SEM micrographs of sample heat treated at 1150°C for 1 h with increasing magnifications from a - d

Grains grew in size above 100 µm and diffusion preceded so fast, that no segregations occurred even after slow furnace cooling (Figure 5a). In higher magnifications micrographs (Figure 5b and 5c) thin cementite layers of submicron thickness are detected (Figure 5c). The very small layers (about 1 µm in thickness) of a microscopically distinguishable phase at grain boundaries is expected to be cementite from morphology comparison, bright SEM BSE contrast, as it is rich in Fe and poor in Si and it is known that quantities as low as 0.002 wt. % in iron-alloys may cause its formation [21]. Albeit the presence of cementite in such low quantities has a negligible effect on the processability and the magnetic properties of the material, its occurrence has to be considered to leave traces in DSC experiments. At higher magnifications (Figure 5d) it is possible to observe ordering domain structures inside the grains similarly to those described in relevant literature of high 6.5 wt. % silicon steel processed by other manufacturing techniques [22, 23]. Depending on whether the centre position of the ordered bcc cell is occupied by Fe atoms and the corner position of Si atoms or the contrary (cp. Figure 1), antiphase domain boundaries exist where two such regions with different stacking order are in contact. The polarization in two adjacent regions with opposite stacking order is also opposed, leading to an increased etching activity at the domain walls that as a consequence are well visible [22]. As ordered domains grow with increasing annealing temperature they become large enough for SEM observation after dwelling at high temperatures such as during A1150 treatment [18].

Calorimetric study

A qualitative overview of occurring signals in heating DSC curves of Fe-Si samples built by SLM is shown by a representative curve in Figure 6.

Figure 6 Observed peaks in DSC heating curves from Fe-Si SLM samples in the as-built condition AsB: the red brackets indicate distinct peaks, the area marked in blue reports fluctuations assigned to the dissolution of Si segregations and cementite, and to SLM process inherent effects

The DSC curve shows four characteristic features, namely, the order transformation of the disordered A2 to the ordered phases B2 +$D0_3$, the magnetic transition, the order-disorder transformation reversing the first ordering transformation, and finally an irregular trend-line, whose features are attributed to a number of normalising diffusion-based mechanisms [24].

It is expected that the as-built samples (AsB) are predominantly disordered in the initial state as the high cooling rates typical of SLM suppress ordering. By heating the material up to the B2+$D0_3$ phase region, an exothermic reaction takes place at 420-580°C. The observed peak in the DSC curve at this temperature can be attributed to the transformation of A2 into B2+$D0_3$ phases, and the associated decrease in entropy as atoms arrange in periodic order. It is also possible that transformation of residual $D0_3$ into B2 occurs in this region, as the latter becomes more stable at higher temperature, superposing the principal order transformation and affecting the peak height shown in the DSC traces.

The magnetic transition, where the atomic spins lose their alignment and the material becomes paramagnetic, occurs at around 680°C [17]. The reversion of the ordering transformation then takes place above 800°C, appearing as a small endothermic second order transition. The peak is shallow as the reaction occurs over a large temperature range.

Turbulences which are located in the region marked by a blue box in Figure 6 are expected to arise from various effects, such as the migration of defects at the cell boundaries, the dissolution of laser segregations, which were observed in Figure 4b and 4c and, at even higher temperatures, cementite dissolution. This leads to a normalizing of a microstructure as noted previously for an austenitic steel built by SLM [24].

Heat treatments affect the volume fraction of the ordered phases in samples and therefore influence the morphology and the temperature range at which the ordering peaks observed in the DSC traces occur. This is shown in Figure 7 where the DSC traces of several specimens, including powder feedstock, as-built and heat treated samples are compared. Similarly Table 4 summaries the temperatures of the peak onset and position caused by the annealing treatments in the B2+DO_3 region.

Figure 7 DSC curves in the region around the disorder-order peak of gas atomized Fe-Si powder, as-built sample and various annealed conditions are plotted

Table 4 Heat treatment and SLM effect on ordering peak

The DSC curve of gas atomized powder (P) shows a broad exothermic peak at 476 ± 4.8°C, corresponding to the transformation from disordered A2 to a more ordered B2 + $D0_3$ structure. As typical for the process, gas atomized powder is assumed to be stress-free, so no superposition between stress effects and no ordering is expected in this specimen. Gas atomized powders

solidify quickly directly from the melt, hence, the maximum possible volume fraction of disordered structure can be attained [25]. The samples in the SLM as-built condition and after partial annealing at 400°C (A400) show an ordering peak with a different morphology compared to that of powder. The ordering peak in these samples has shifted to higher temperatures, 528.7 ± 3.8°C and 534.9 ± 2.4°C respectively, and decreased in size. These shifts demonstrate that the samples in the AsB or A400 conditions have a structure less disordered than that of the powder feedstock. A partial ordering in the as-built parts could arise from the repeated exposure to the laser during the layer-to-layer process, causing heat introduction from adjacent built layers and reheating. Similarly, annealing treatments in the low portion of the B2+$D0_3$ region, such as A400, might induce some structural ordering, as indicated by a smaller peak, and retardation in the ordering reaction (Figure 7).

The onset temperature for ordering is not definitively established in the literature as ordering depends on diffusion and hence, on both temperature and time. It is believed that at 400°C diffusion is slow [20, 26] and ordering might only occur partially, in specific regions of the material, for example close to defects where diffusion is accelerated or in correspondence of the transformation of the metastable B2 into B2+DO_3. By prolonging the dwell time at 400°C (Ex400) different ratios of B2 to $D0_3$ might form but still the heat treatment did not lead to a complete ordering as indicated by the fact that the ordering peak diminishes in size and occurs at even higher temperatures (576.6 ± 7.7°C).

The ordering peak vanishes entirely in the DSC traces of the samples treated in the high portion of the B2+$D0_3$ region or above. This indicates that the disordered phases A2, and any excess B2 present in the as-built condition, transform fully into equilibrium structures when annealing in these conditions. No significant differences in the peak are observed for A620 and A1150, demonstrating that after annealing for 1 h at 620°C the ordering reactions have completed. The DSC traces of all samples annealed and furnace cooled above 620°C present a shallow endothermic peak. It is expected that this might derive the partial conversion of DO_3 into B2 as temperature increases as B2 is more stable at higher temperatures.

It is noteworthy that no antiphase domains were found in the SEM analysis except in the sample treated in the high portion of the A2 region (A1150). This is possibly because the ordered domains created at lower temperatures are too small to be detected at least by the microscopy techniques used in this research.

Figure 8 also shows detail of the DSC traces of samples that were treated in the B2 (Q700) and A2 (Q900) and then water quenched.

Figure 8 DSC heating curves of as-built, water quenched and furnace cooled at the same temperatures conditions

Quenching from the B2 or A2 phase region leads to a partially disordered state as both curves show distinct peaks. No significant difference in peak magnitude can be observed in these conditions (Q700 and Q900, which should "freeze" the B2 and A2, structures according to the phase diagram [7]. Similar to the cases of the as-built and low temperature annealed samples, it is believed that the ordering peak for the samples in these conditions is showing mainly the conversion of the A2 and/or B2 phase into B2+DO_3 phases. The fact that these exothermic peaks are smaller than that observed for the as-built condition suggests that SLM can hinder ordering more effectively than water quenching, perhaps due to the fact that solidification occurs at even higher cooling rates.

It is noteworthy that the heat treatments conducted in the B2 (Q700) and A2 (Q900) phase regions neither modify the magnetic transformation nor have an impact on the reversion of the ordering transformation that occurs above 800°C as all samples whether initially ordered or not, the specimens become ordered at these temperatures.

Hardness results

According to a related research on hardness variation of quenched silicon ribbons subjected to various heat treatments [17], the volume fraction of the ordered phase influences hardness significantly. For this reason, the hardness of the samples in the different conditions presented in this study was also compared. The results of hardness measurements for specimen of all conditions are presented in Figure 9.

Figure 9 Vickers Hardness of samples: black squares represent samples in 1 h annealed conditions AsB and A400-A1150, red dots represent samples with either extended dwell time or quenched conditions Ex400, Ex620, Q700 and Q900. Error bars are also shown in the image.

Figure 9 shows that the hardness of samples as-built (AsB) is about 373.46 ± 11.91 HV. It was observed that the sample hardness does not change when the as-built specimens are heat treated in the low portion of the B2+DO_3 region. As indicated by the analysis of the corresponding DSC traces and now reinforced by the found hardness values, heat treating at low temperature appears to cause a conversion of the metastable B2 into DO_3 phase and is only responsible for a

negligible ordering transformation of the disordered phase. The comparison of the hardness of the samples in the as-built condition and A400 and Ex400 also indicates that residual stresses, which should have been partially released during the heat treatment, do not affect the hardness significantly.

The hardness of the material changes markedly when heat treated in the high portion of the B2+DO_3 and B2 phase regions. Indeed, the samples subjected to the A620 and A700 heat treatments exhibit hardness above 420 HV and up to 430 HV, respectively. This increase in hardness is likely to be related to the formation of ordered domains at these high temperatures. In confirmation, the sample heated to 620°C for 5 h (Ex620) shows a similar hardness to that treated at the same temperature or above for 1 h (A620 and A700), suggesting that after 1 h at 620°C the ordering transformation is complete, as expected from the DSC curves.

Figure 9 also shows that the hardness values of the samples obtained from annealing in the B2 region and then cooled by furnace cooling or quenching are similar. This is a surprising result, as the samples in these conditions have a similar volume fraction of disordered phase but different ratio of B2 and DO_3 ordered phases and according to the literature should possess different hardness. This difference could be related to the morphology of the ordered phases, as it has been shown in previous work that, based on processing and thermal history, the morphology of ordered phases can differ and may contribute to a variation in hardness [13,14] .

In contrast, a marked difference between the hardness of samples obtained from annealing in the A2 region and then cooled in the furnace or quenched is observed. The quenched specimens annealed in the A2 region have a hardness similar to that of the as-built samples, whereas the samples that are furnace cooled have a high hardness similar to that obtained upon slow cooling the material from the high portion of the B2+$D0_3$ or B2 phase regions. This confirms indeed that hardness is mainly affected by the volume fraction of the ordered phases at room temperature and that after quenching the samples from the A2 region, a certain amount of metastable ordered phase is retained at room temperature.

Finally, annealing the samples at 1150°C (high portion of the A2 region) followed by furnace cooling leads to intermediate hardness values between those found for the as-built and A700 and A620 conditions. It is likely that this decrease in hardness derives from the significant microstructural evolution of the samples that showed dissolution of the SLM typical fine cellular structures and grain growth.

The combination of DSC analysis and hardness testing cannot provide an absolute quantitative measure of the amount of ordering, but as shown in this study, provides useful insights to understand the ordering reactions in high silicon steel. In this research work it was shown that SLM can be used to produce Fe-Si components with mainly disordered microstructures thanks to the fact the material is shaped point by point in small amounts at the time, surmounting the manufacturing problems associated to ordering and material embrittlement.

The additive manufactured high silicon steel components are printed in their net-shape and therefore do not require thermo-mechanical post-processing. However, in this work it was shown how it is possible to manipulate the microstructure of the as-printed parts by heat treatments that can modify the grain size and cancel the undesired inhomogeneities induced by the laser processing. Although it is recognised that ordering leads to material embrittlement, its effect on the magnetic properties is not well understood. As part of future works the relationship between the microstructure of the printed (and heat treated) parts and the magnetic properties will be investigated to assess whether SLM can be used as an effective manufacturing route for the production of high silicon steel for advanced applications.

Conclusions

In this work, a microstructural and calorimetric study of high silicon Fe-Si parts built by SLM is presented. It is demonstrated that the ordering state of the material depends on the thermal history introduced by the manufacturing process and the post-processing annealing heat treatments. The following conclusions can be drawn from the microstructure, DSC and hardness investigations:

- It has been shown that DSC can be used as a means to study ordering in high-silicon steel processed by SLM. Ordering reactions can be assigned to two distinct features in DSC traces. Calorimetry results have been corroborated using microscopy and micro-hardness measurements;

- The study of the effects of different heat-treatment conditions on the microstructures of SLM high-silicon steel has shown that ordered phases of type B2 and $D0_3$ form inside the grains in proportions determined by the heat-treatment temperature, dwell time and

cooling rate. In particular, when cooling is sufficiently slow (i.e. furnace cooling) the ordering transformation takes place as predicted by the phase diagram of Fe-Si;

- Various heat treatments were exploited to modify the microstructure of parts built by SLM. The onset temperature for micro-segregation dissolution was found to be around 700°C, the onset temperature for grain growth around 900°C. After annealing at 1150°C for one hour grains grow above 100 µm, therefore close to the saturation size [10]. Annealing in the high portion of the A2 leads to a marked grain growth;

- In order to avoid extensive ordering, rapid cooling can be performed from temperatures in the A2 phase region. In this regard, SLM-processing and water-quenching are two effective means to supress partially the ordering transformation. Annealing of parts built by SLM with subsequent quenching could be a promising strategy for the production of parts with a more homogeneous microstructure, more suitable for magnetic applications;

- By shedding light on the phase-ordering mechanisms and the effect of heat treatments on microstructure of high-silicon steel built by SLM, the present study paves the way towards the optimisation of the mechanical and magnetic properties of this alloy.

Acknowledgements

The research leading to these results has received partial funding from the People Programme (Marie Curie Actions) of the European Union's Seventh Framework Programme (FP7/2007-2013) under REA grant agreement no 608322 as well as receiving support from the UK Engineering and Physical Sciences Research Council (EPSRC) through the grant EP/I033335/2 "EPSRC Centre for Innovative Manufacturing in Additive Manufacturing".

References

[1] M. Komatsubara, K. Sadahiro, O. Kondo, T. Takamiya, A. Honda, Newly developed electrical steel for high-frequency use, Journal of Magnetism and Magnetic Materials, 242–245 (2002) 212-215

[2] H. Ninomiya, Y. Tanaka, A. Hiura, Y. Takada, Magnetostriction and applications of 6.5% Si steel sheet, Journal of Applied Physics, 69 (1991) 5358-5360

[3] H. Honma, Y. Ushigami, Y. Suga, Magnetic properties of (110)[001] grain oriented 6.5% silicon steel, Journal of Applied Physics., 70 (1991) 6259-6261

[4] K.-I. Arai, N. Tsuya, Ribbon-Form Silicon-Iron Alloy Containing Around 6.5 Percent Silicon, IEEE Transactions on magnetics, 16 (1980) 126-129

[5] X. D. He, X. Li, Y. Sun, Microstructure and magnetic properties of high silicon electrical steel produced by electron beam physical vapor deposition, Journal of Magnetism and Magnetic Materials, 320 (2008) 217-221

[6] R. D. Cava, W.J. Botta, C.S. Kiminami, M. Olzon-Dionysio, S.D. Souza, A.M. Jorge Jr., C. Bolfarini, Ordered phases and texture in spray-formed Fe–5 wt%Si, Journal of Alloys and Compounds, 509 (2011) 260-264

[7] P. R. Swann, L. Grånäs, B. Lehtinen, The B2 and DO3 Ordering Reactions in Iron–Silicon Alloys in the Vicinity of the Curie Temperature, Metal Science, 9 (1975) 90-96

[8] F. González, Y. Houbaert, A review of ordering phenomena in iron-silicon alloys, *Revista De Metalurgia*, 49 (2013) 178-199

[9] W. J. Yuan, R. Li, Q. Shen and L. M. Zhang, Characterization of the evaluation of the solid solubility of Si in sintered Fe–Si alloys using DSC technique, Materials Characterization, 58 (2007) 376-379

[10] K. Narita, M. Enokizono, Effect of Ordering on Magnetic Properties of 6.5-Percent Silicon-Iron Alloy, IEEE Transactions on Magnetics, 15 (1) (1979) 911-915

[11] P. Jang, B. Lee, G. Choi, Effects of annealing on the magnetic properties of Fe–6.5%Si alloy powder cores, Journal of Applied Physics, 103 (2008)

[12] M. Garibaldi, I. Ashcroft, M. Simonelli, R. Hague, Metallurgy of high-silicon steel parts produced using Selective Laser Melting, Acta Materialia, 110 (2016) 207-216

[13] Y. Ustinovshikov, I. Sapegina, Morphology of ordering FeSi alloy, Journal of Materials Science, 39 (2004) 1007-1016

[14] J.S. Shin, J.S. Bae, H.J. Kim, H.M. Lee, T.D. Lee, E.J. Lavernia, Z.H. Lee, Ordering–disordering phenomena and micro-hardness characteristics of B2 phase in Fe–(5–6.5%)Si alloys, Materials Science and Engineering A, 407 (2005) 282-290

[15] T. Ros-Yanez, D. Ruiz, J. Barros, Y. Houbaert, R. Colas, Study of deformation and aging behaviour of iron–silicon alloys, Materials Science and Engineering A, 447 (2007) 27-34

[16] D. Ruiz, T. Ros Yañez , G.J. Cuello , R.E. Vandenberghe , Y. Houbaert, Order in Fe–Si alloys: A neutron diffraction study, Physica B, 385-386 (2006) 578-580

[17] M. Abdellaoui, T. Barradi, E. Gaffet, Mechanism of mechanical alloying phase formation and related magnetic and mechanical properties in the Fe-Si system, Journal of Alloys and Compounds, 198 (1993) 155-164

[18] F. Faudot, J. F. Rialland, J. Bigot, Study of Order-Disorder Effect on Magnetic Properties of Rapidly Quenched Fe-6.5 wt.% Si Alloys, Physica Scripta, 39 (1989) 263-267

[19] ASTM 52921:2013(E) -Standard Terminology for Additive Manufacturing—Coordinate Systems and Test Methodologies, ASTM International, 25 W. 43rd St., 4th Floor, New York, NY 10036 (2016)

[20] H. Oikawa, Review of Lattice Diffusion of Substitutional Impurities in Iron. A Summary Report, Tech. Reports, Tohoku Univ., 47 (1982) 215

[21] K. Shibata, K. Asakura, Transformation Behavior and Microstructures in Ultra-low Carbon Steels, ISIJ International, 35 (1995), 982-991

[22] P. R. Potnis, N.-T. Tsou, J. E. Huber, A Review of Domain Modelling and Domain Imaging Techniques in Ferroelectric Crystals, Materials, 4 (2011) 417-447

[23] H. Fu, Q. Yang, Z. Zhang, J. Xie, Effects of precipitated phase and order degree on bending properties of an Fe-6.5 wt%Si alloy with columnar grains, Journal of Materials Research, 26 (2011) 1711-1718

[24] K. O. Bazaleeva, E. V. Tsvetkova, E. V. Balakirev, I. A. Yadroitsev, I. Y. Smurov, Thermal Stability of the Cellular Structure of an Austenitic Alloy after Selective Laser Melting, Russian Metallurgy (Metally), 5 (2016) 424-430

[25] A. M. Mullis, L. Farrell, R. F. Cochrane, N. J. Adkins, Estimation of Cooling Rates During Close-Coupled Gas Atomization Using Secondary Dendrite Arm Spacing Measurement, Metallurgical and Materials Transactions B, 44 (2013) 992–999

[26] A. Gude, H. Mehrer, Diffusion in the $D0_3$-type intermetallic phase Fe_3Si, Phylosophical Magazine A, 76 (1997) 1-29

Table 1 Composition of Fe-Si powders

Fe-Si	*Si*	*C*	*Mn*	*P*	*O*	*Fe*
wt. %	6.9	0.01	0.05	0.009	0.0065	Bal.

Table 2 Selected build parameters for processing of Fe-Si cubic specimens

Power	P [W]	70
Scan speed	v [mm/s]	500
Focal position	Δz [mm]	13.1
Hatch spacing	d_h [µm]	60
Layer thickness	l_t [µm]	25

Table 3 Overview of the investigated Fe-Si samples. The cooling method, annealing temperature, dwell time and the region of the phase diagram covered by the heat treatment are presented in the Table.

Code	*Sample type*	*Cooling*	*T [°C]*	*Heat treated in phase region*	*Dwell time[h]*
P	Gas atomized powders	As-received	-	-	-
AsB	SLMed 5 × 5 × 5 mm cube	As-built	-	-	-
A1150	SLMed 5 × 5 × 5 mm cube	Furnace cooled	1150	A2	1
A400	SLMed 5 × 5 × 5 mm cube	Furnace cooled	400	B2+DO_3	1
Ex400	SLMed 5 × 5 × 5 mm cube	Furnace cooled	400	B2+DO_3	24
A700	SLMed 5 × 5 × 5 mm cube	Furnace cooled	700	B2	1

Q700	SLMed 5 × 5 × 5 mm cube	Water quenched	700	B2	1
A620	SLMed 5 × 5 × 5 mm cube	Furnace cooled	620	B2+DO_3	1
Ex620	SLMed 5 × 5 × 5 mm cube	Furnace cooled	620	B2+DO_3	5
A900	SLMed 5 × 5 × 5 mm cube	Furnace cooled	900	A2	1
Q900	SLMed 5 × 5 × 5 mm cube	Water quenched	900	A2	1

Table 4 Heat treatment and SLM effect on ordering peak

Condition	***Peak Onset [°C]***	***Peak Position [°C]***
P – Powder	302.7 ± 5.5	476.6 ± 4.8
AsB - As built	383.5 ± 6.5	518.7 ± 3.8
A400 - 400°C, 1 h	454.7 ± 2.8	534.9 ± 2.5
Ex400 - 400°C, 24 h	496.0 ± 2.8	567.95 ± 7.7

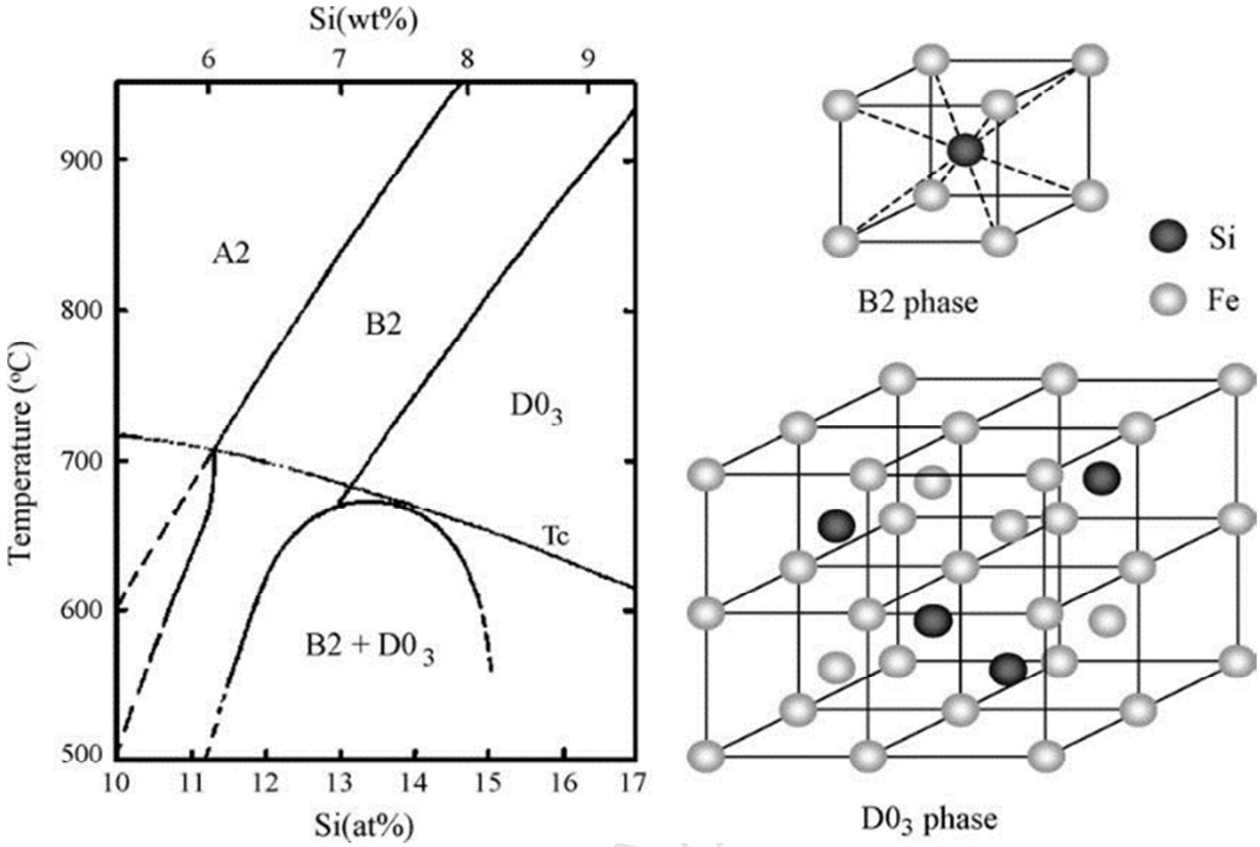

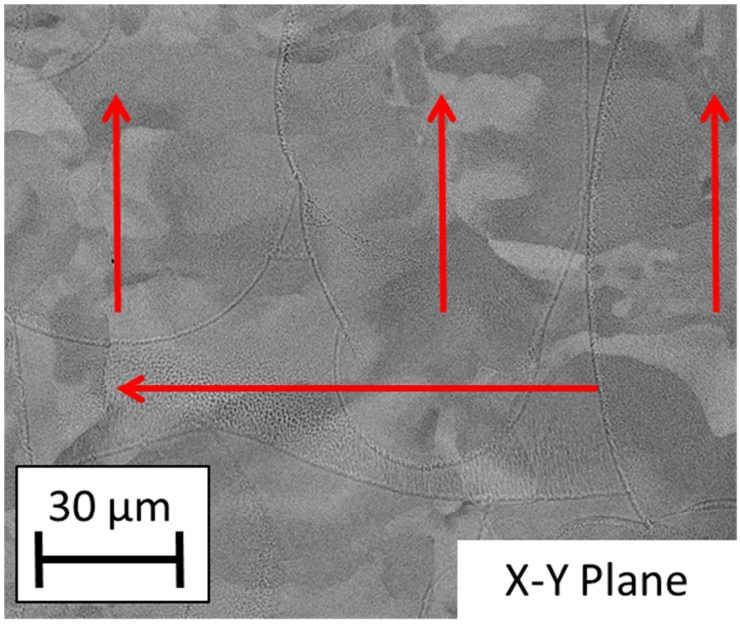

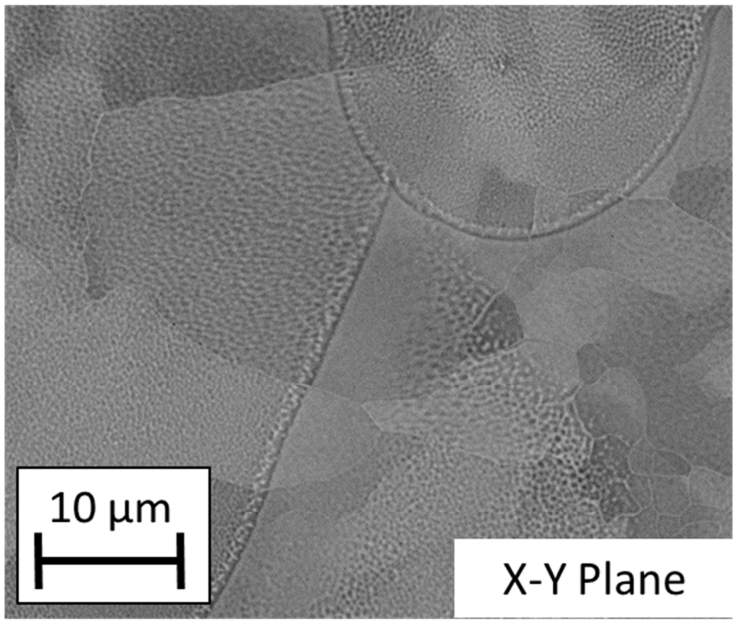

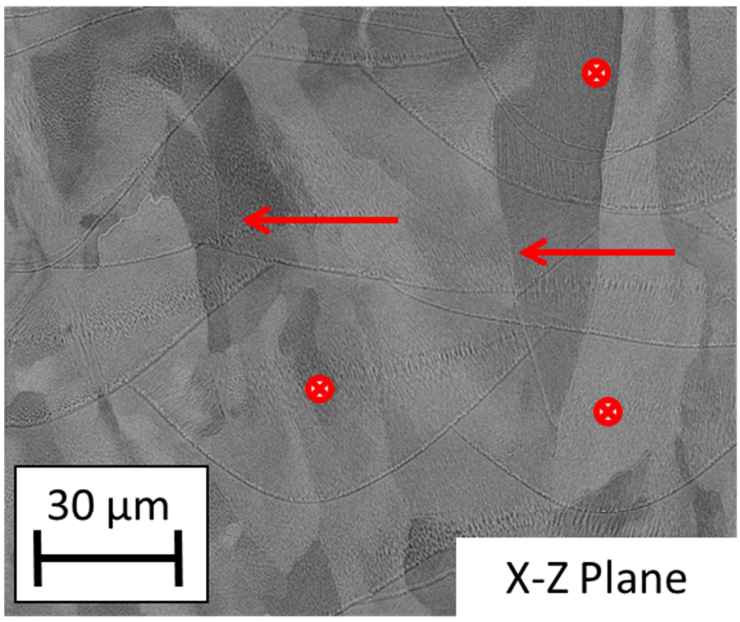

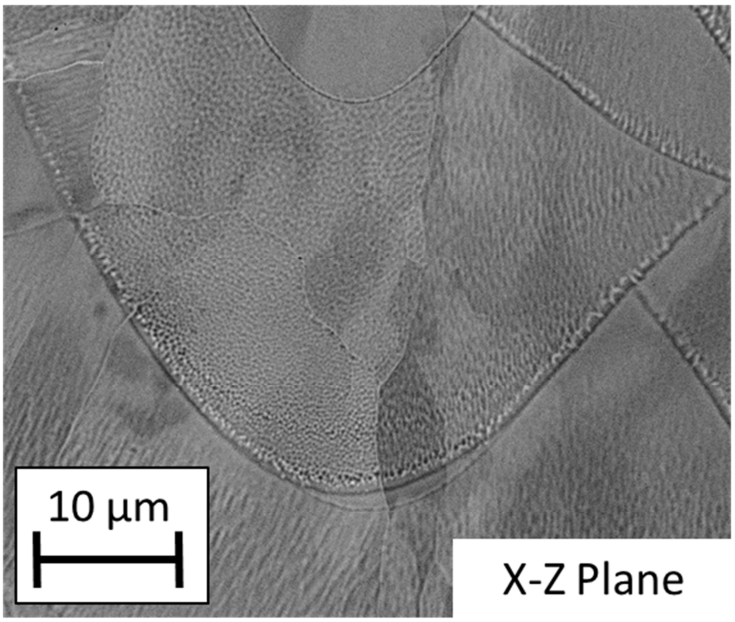

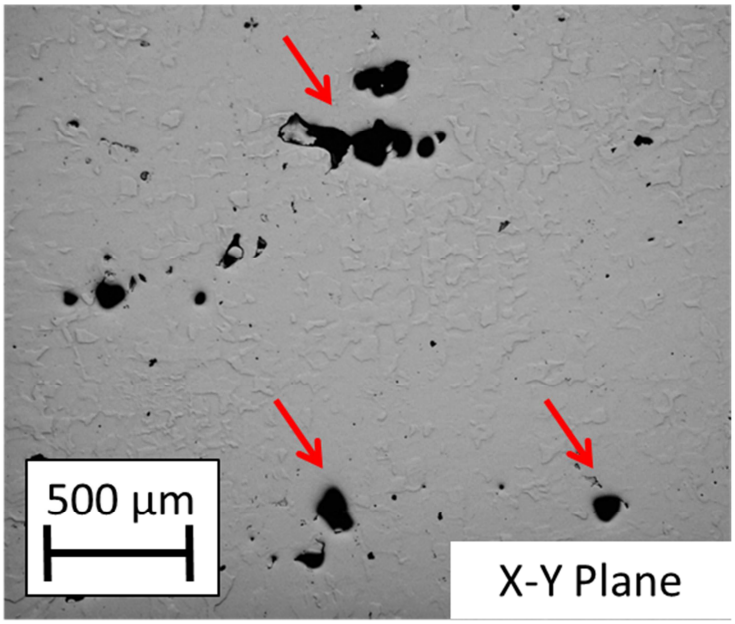

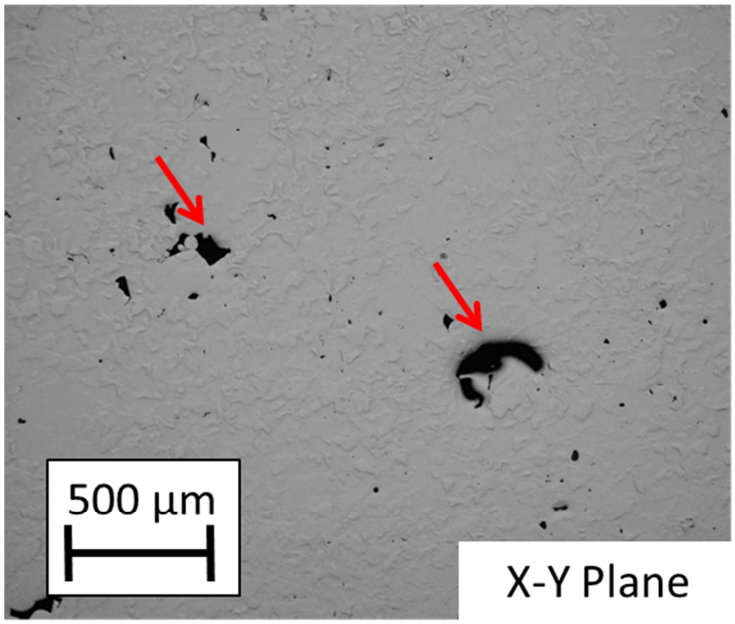

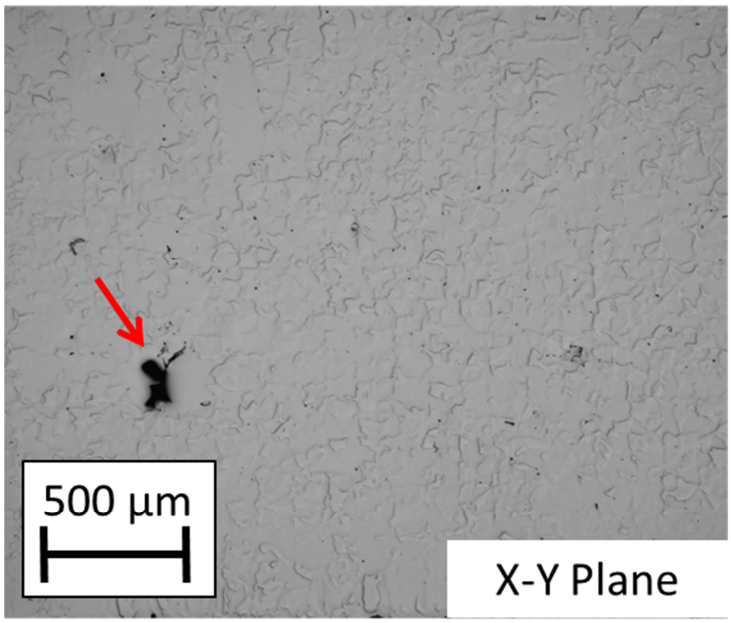

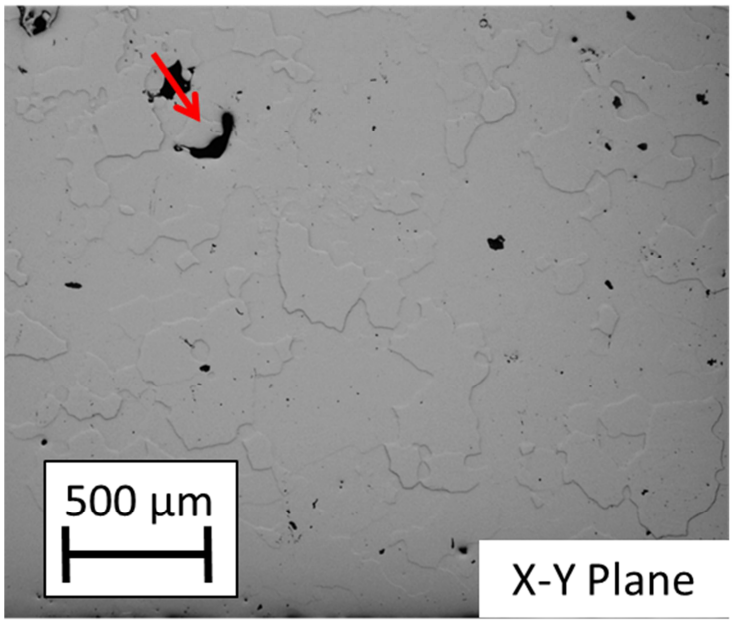

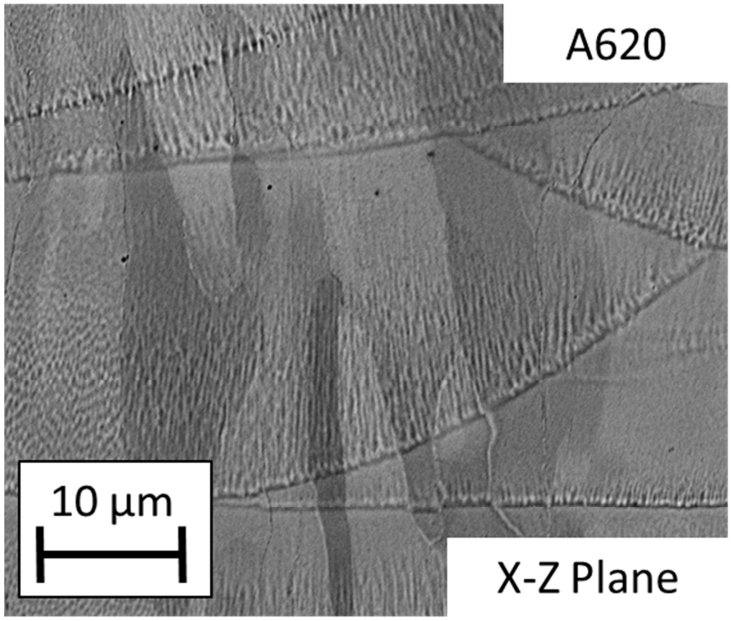

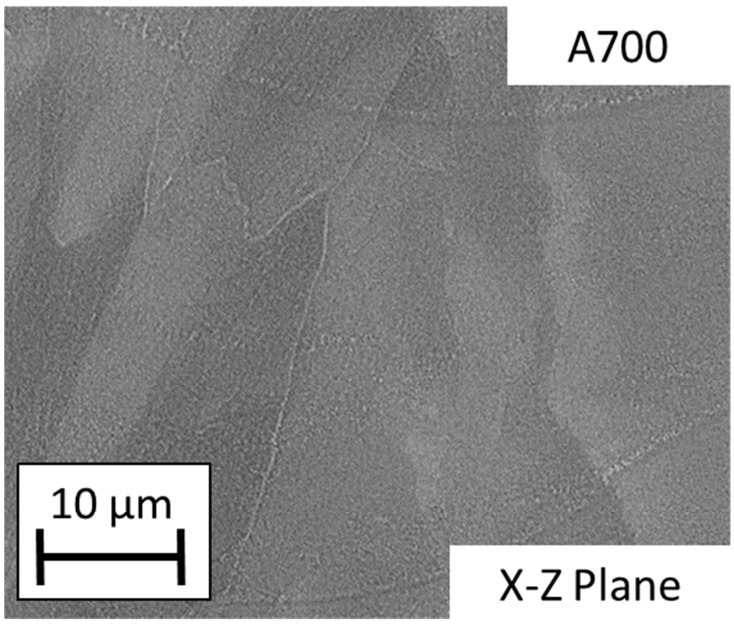

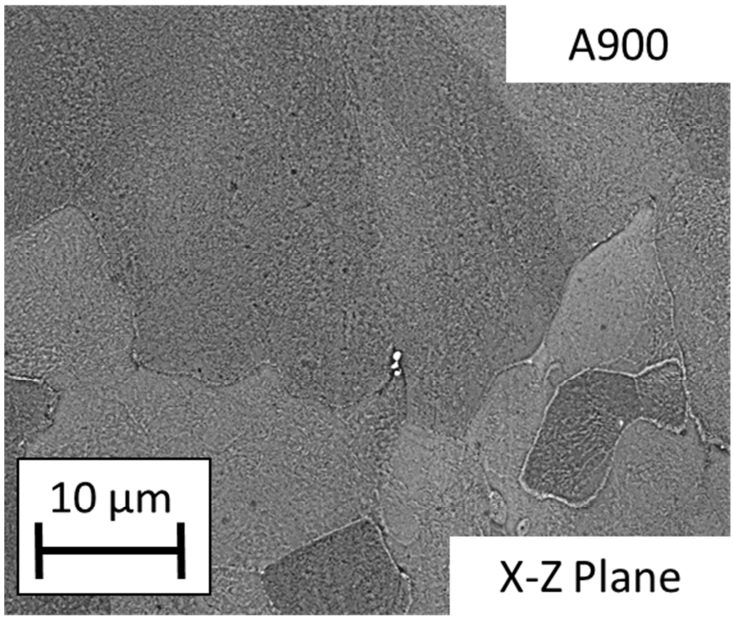

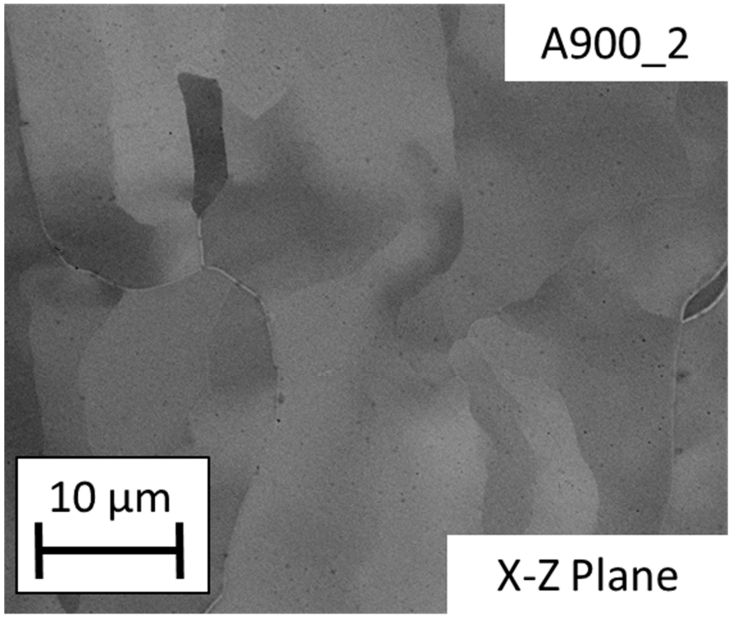

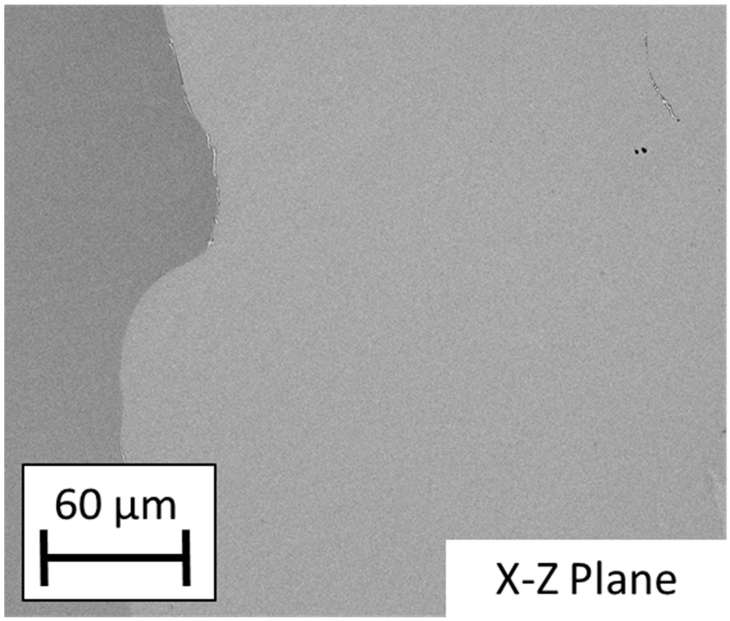

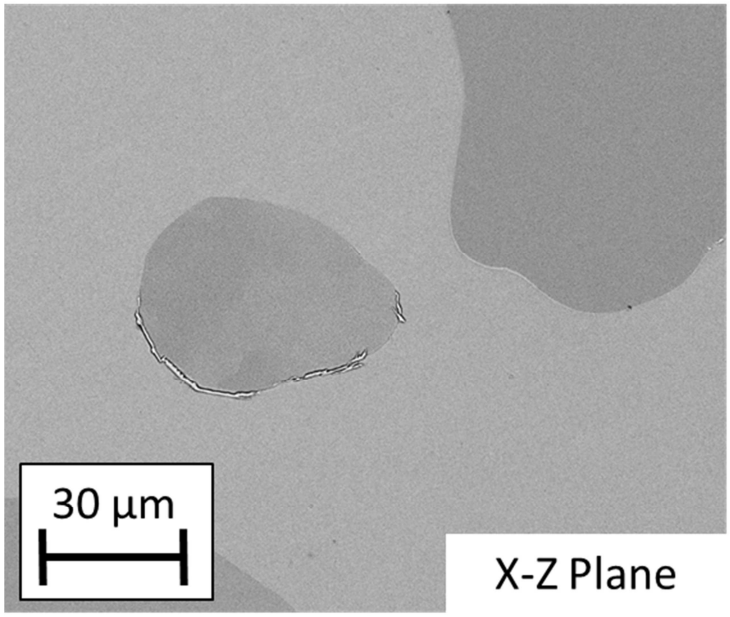

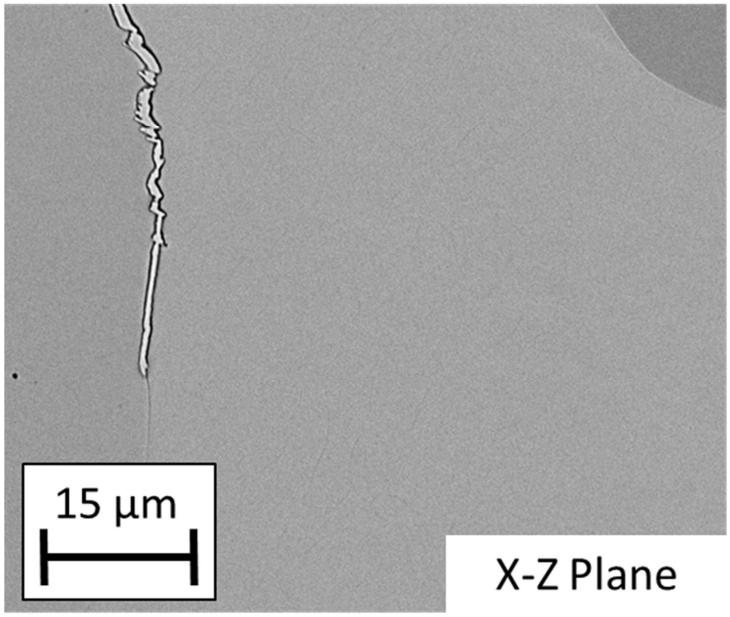

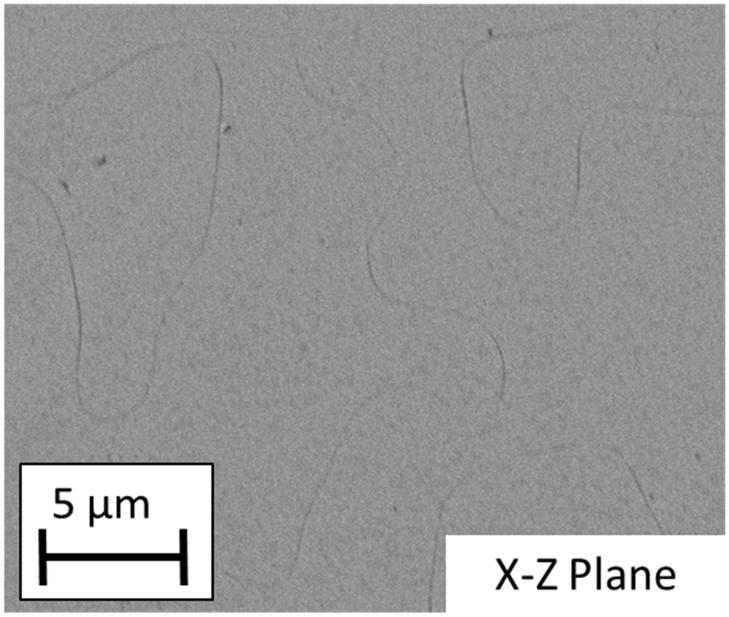

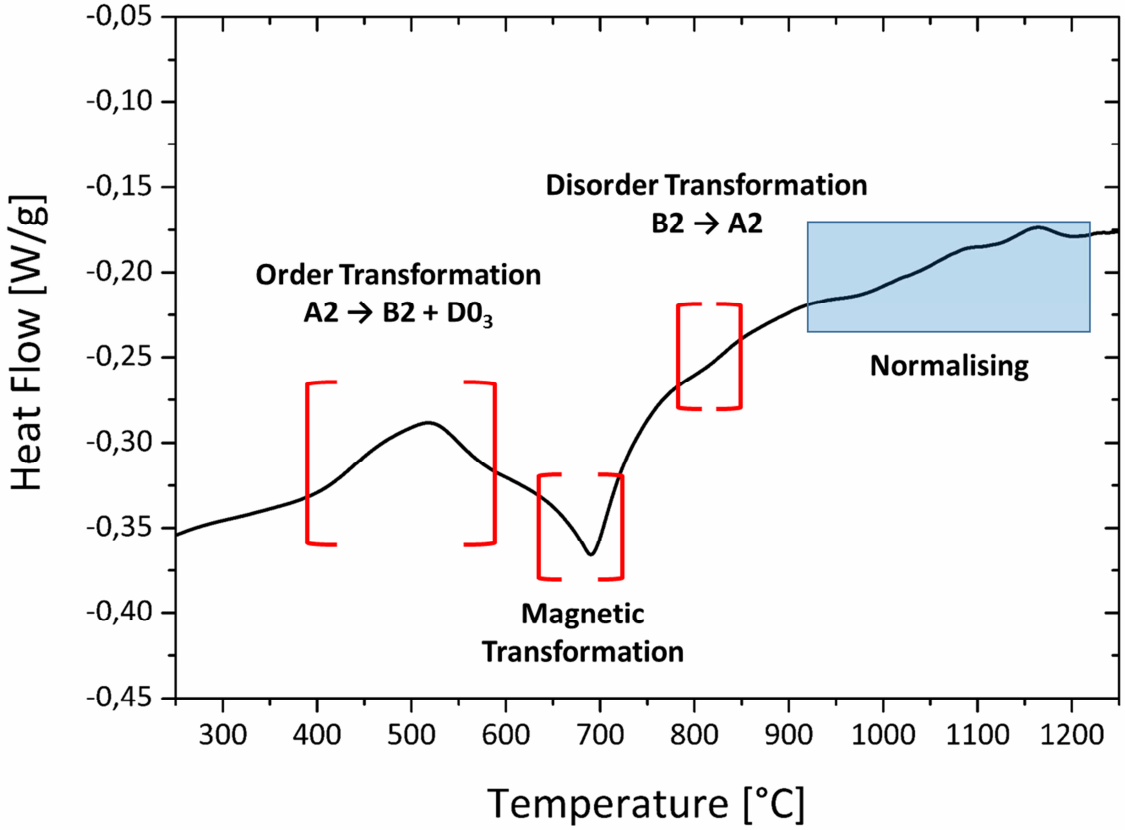
-0,05
-0,10
-0,15
-0,20
-0,25
-0,30
-0,35
-0,40
-0,45
Heat Flow [W/g]
300
400
500
600
700
800
900
1000
1100
1200
Temperature [°C]
Disorder Transformation
B2 → A2
Order Transformation
A2 → B2 + D0$_3$
Normalising
Magnetic
Transformation

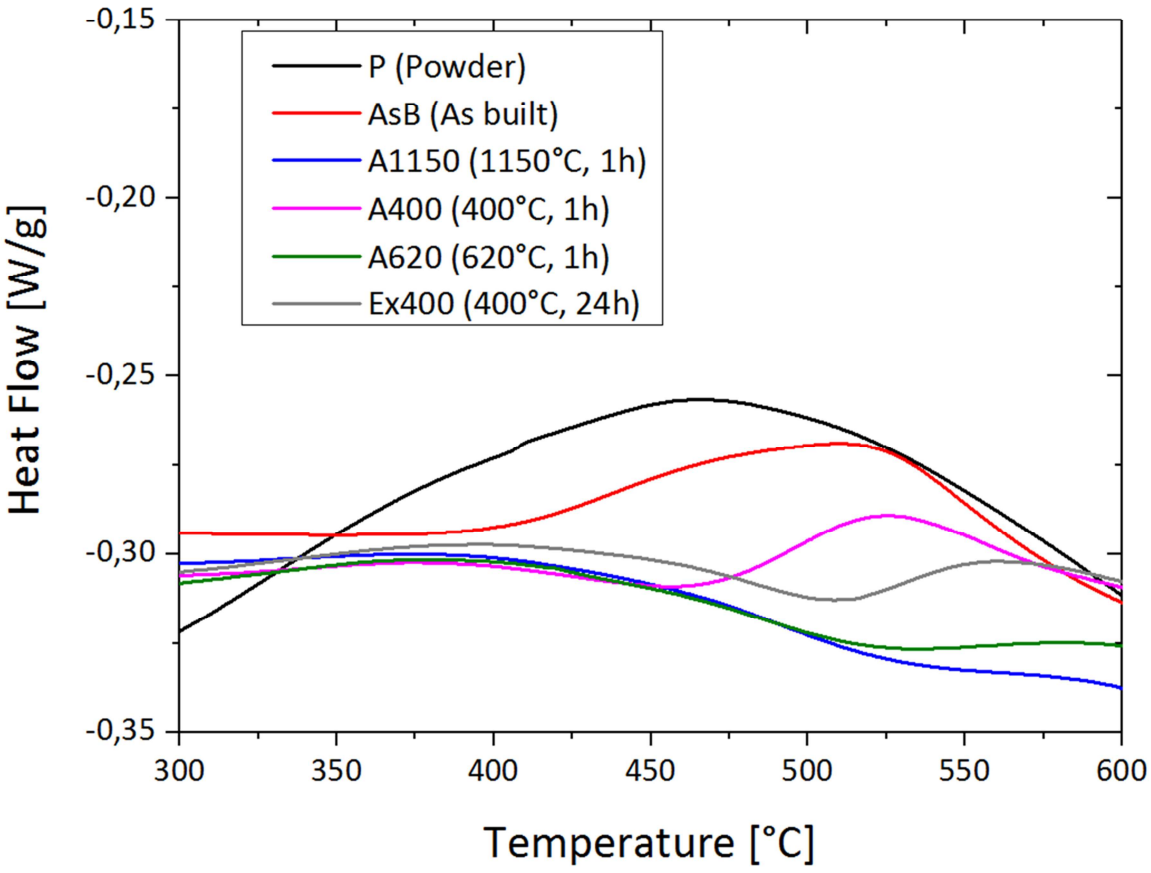
P (Powder)
AsB (As built)
A1150 (1150°C, 1h)
A400 (400°C, 1h)
A620 (620°C, 1h)
Ex400 (400°C, 24h)
Heat Flow [W/g]
-0,15
-0,20
-0,25
-0,30
-0,35
300
350
400
450
500
550
600
Temperature [°C]

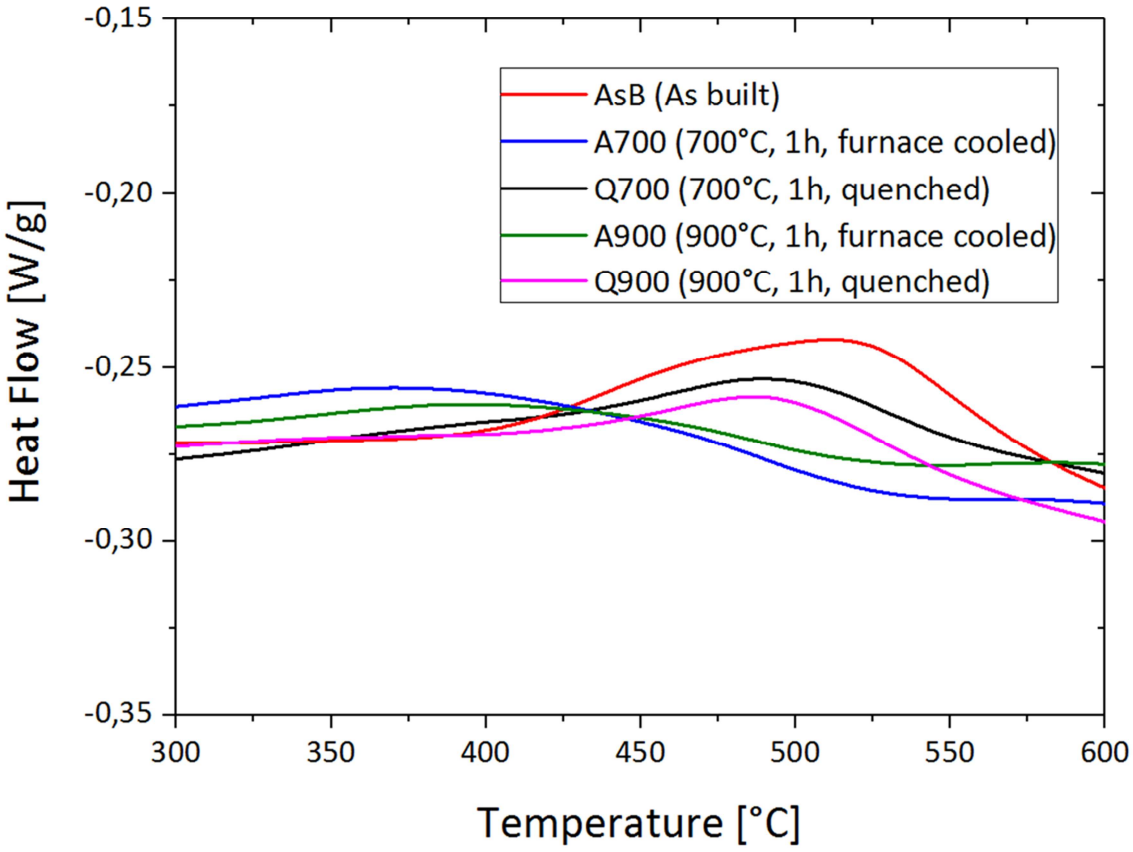
-0,15
-0,20
-0,25
-0,30
-0,35
Heat Flow [W/g]
300
350
400
450
500
550
600
Temperature [°C]
AsB (As built)
A700 (700°C, 1h, furnace cooled)
Q700 (700°C, 1h, quenched)
A900 (900°C, 1h, furnace cooled)
Q900 (900°C, 1h, quenched)

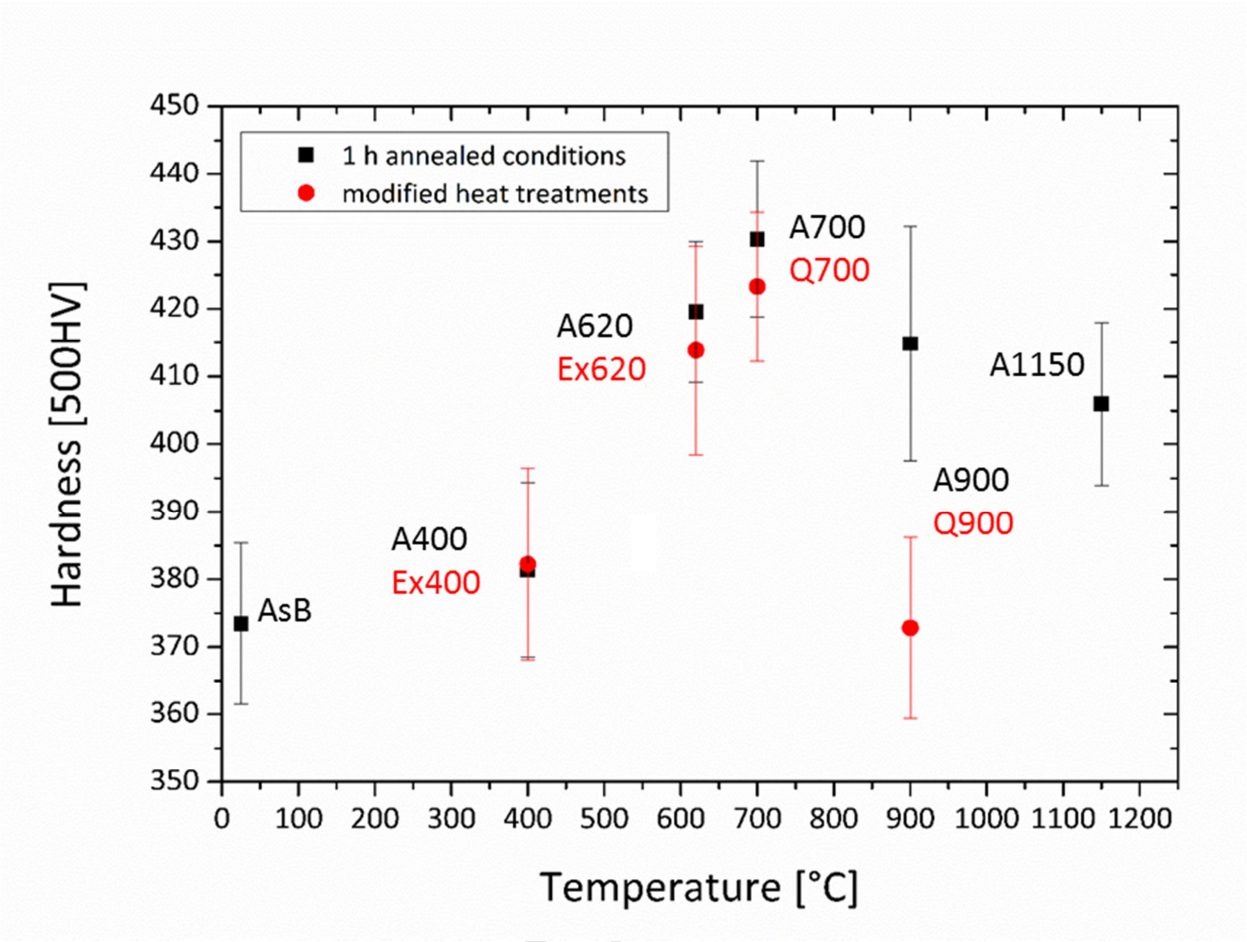
1 h annealed conditions
modified heat treatments
AsB
A400
Ex400
A620
Ex620
A700
Q700
A900
Q900
A1150
Hardness [500HV]
Temperature [°C]
450
440
430
420
410
400
390
380
370
360
350
0
100
200
300
400
500
600
700
800
900
1000
1100
1200

Microstructural ordering in high-silicon steel processed by SLM is characterized

Ordering in FeSi built by SLM is assigned to curve features in DSC measurements

Heat treatments in order to tailor the microstructure of SLMed FeSi are presented